IMPLICATION FOR SUBSURFACE SCATTERING STRUCTURE NEAR APOLLO 12 LANDING SITE FROM SEISMIC WAVE PROPAGATION SIMULATION. K. Onodera[1,2], T. Kawamura[1], S. Tanaka[3], Y. Ishihara[4], and T. Maeda[5], [1]Institut de Physique du Globe de Paris / Université de Paris, 35 rue Hélène Brion, 75205, Paris, France (onodera@ipgp.fr), [2]The Graduate University for Advanced Studies (SOKENDAI), 3-1-1 Yoshinodai, Chuo-ku, Sagamihara, Kanagawa 252-5210, Japan, [3]Institute of Space and Astronautical Science, Japan Aerospace Exploration Agency, 3-1-1 Yoshinodai, Chuo-ku, Sagamihara, Kanagawa 252-5210, Japan, [4]National Institute for Environmental Studies, 16-2 Onogawa, Tsukuba-shi, Ibaraki 305-8506, Japan, [5]Hirosaki University, 3 Bunkyo-cho, Hirosaki-shi, Aomori 036-8561, Japan.

Introduction: The internal structure of the Moon has been investigated using the seismic data obtained in the Apollo missions. So far, several 1-D inner structure models have been proposed (e.g. [1]-[3]). However, these models show some discrepancies and sometimes the differences exceed their error bars, implying we can interpret the lunar interior in some different ways even if the similar data set is used. One of the most serious problems is the intense scattering which keeps us from a precise determination of arrival times of seismic waves, leading to a large error in a resulting structure model. As for the lunar seismic scattering, the subsurface fractured layers called regolith and megaregolith is considered to have a strong contribution [4]. Therefore, understanding the scattering structure of the lunar subsurface will be a key to improve our knowledge of the internal structure of the Moon.

The objective of this study is to constrain the subsurface scattering structure by conducting seismic wave propagation simulations under different structure settings and comparing synthetics with the Apollo seismic data.

Simulated Seismic Events: This study focused on the Apollo artificial impacts because of their well-constrained impact locations, origin times and impact parameters. Since the OpenSWPC [5], which is a simulation code used in this study, dealt with only Cartesian coordinate system, we selected the artificial impacts having the epicentral distance less than 300 km (~10 deg) beyond which the influence of curvature clearly shows up. In addition, Lunar Module (LM) impacts were excluded. Since these are very oblique impacts (< 10 deg from the horizon), we considered it would be difficult to model the seismic source for LM impacts. Therefore, 3 events from Saturn IVB (S-IVB) impacts whose impact angles are closer to 90 deg than LM ones were selected (Table 1). Note that Apollo 13 S-IVB impact was ruled out due to its saturation around energy peak.

Table 1. Selected Apollo Artificial Impacts

S-IVB impact	Seismic Station	Distance (km)
Apollo 16	Station 12	153.7
Apollo 14	Station 12	175.3
Apollo 15	Station 14	185.5

Inputs for Simulations: As for velocity structure, we constructed 2 models basically referring to VPREMOON [3] (Table 2). Note that the different V_p/V_s ratio was given for each case. One was referred from the experimental results on the Apollo 12 samples by Kanamori et al. (1971) [6] (V_p/V_s ratio = 1.59, 1.82 for regolith and megaregolith), while the other was determined based on the results of the lunar seismic wave simulations by Onodera et al. (2019) [7] (V_p/V_s ratio = 1.25, 1.39 for regolith and megaregolith, which correspond to that of very dry samples on earth [8][9]). Since random media was inserted in the regolith and the megaregolith layer, the seismic velocity within these layers fluctuated about 28 and 14% respectively. The typical scale of the random media was set to 200 m for the regolith and 600 m for the megaregolith [4]. Intrinsic Q was given from the results by the previous studies [3][4][10].

Table 2. Velocity Structure Models
*Since the random media was inserted in the regolith and the megaregolith layer, the seismic velocities fluctuate by 28 and 14% respectively in each layer.

Layer	Kanamori1979		Onodera2019		Intrinsic Q	
	V_p (km/s)	V_s (km/s)	V_p (km/s)	V_s (km/s)	Q_p	Q_s
Regolith	1.38*	0.80*	1.38*	0.87*	6750	6750
Megaregolith	3.20*	1.76*	3.20*	1.76*	5000	5000
Crust	5.50	3.18	5.50	3.18	4000	4000
Mantle	7.55	4.36	7.55	4.36	3750	1500

In addition to the random media, we introduced topographies in our simulations because these are considered to have an influence on the development of scattering as well [4][5]. For the crustal structure, we adopted Model 2 of Wieczorek et al. (2013) [11] which was constructed from the GRAIL gravity data combined with the Apollo seismic data, producing the average crustal thickness of 35 km. In order to evaluate how the envelope grows under different structure settings for scattering layer, we prepared 6 different scattering structure models (Table 3). In the models, the regolith-megaregolith boundary depth varies from 2.5-7.5 km whereas megaregolith and crust boundary depth does from 10-20km.

Table 3. Regolith and Megaregolith Structure Models
K represents Kanamori1979 velocity model and O shows Onodera2019 model.

Model (X = K or O)	Regolith boundary (km)	Megaregolith boundary (km)
Model X-1	2.5	10
Model X-2	5.0	10
Model X-3	7.5	10
Model X-4	2.5	20
Model X-5	5.0	20
Model X-6	7.5	20

We assumed an isotropic radiation of P-wave as a seismic source and Kupper wavelet with excitation time of 0.65 s as a source time function [7].

Under these conditions, the simulations were performed in 2-D P-SV system along each event's path. Since, in the OpenSWPC [5], the amplitude of 2-D simulation outputs is not precise as much as 3-D ones, all seismic waveforms were basically normalized in the analysis.

For the comparison between the simulated waves and the Apollo data, all seismic signals were converted into velocity unit, and the same bandpass filter (0.2 – 1.5 Hz [7]) was applied, allowing us to compare the simulated waves and the Apollo data in the same physical unit and frequency band. We especially focused on the build-up of the scattering coda (i.e. from the wave arrival to the energy peak) which strongly reflect the scattering properties [12]. In the analyses, each seismic envelope was smoothed with time window of 7.5 s, and we compared the synthetics and the real data from the viewpoint of rise time and seismic energy, and evaluated which structure model is the best to explain the Apollo data.

Results and Discussions: We firstly looked into the rise time to investigate whether each velocity model can explain the Apollo data. In Figure 1, while filled colored-symbols correspond to the rise times of Kanamori1971 velocity model, open ones to those of Onodera2019 model. Overall, the rise times for Onodera2019 model show better agreement with those of the Apollo especially in the case of Apollo 14 S-IVB observed at Station 12 (hereafter termed like A14S12). This means that the smaller V_p/V_s ratio is more appropriate than those by the previous studies in order to model the rise time arrival of the Apollo. In fact, since the ratio of Onodera2019 model represents an extremely dry condition, this result seems consistent with the unique environment on the Moon.

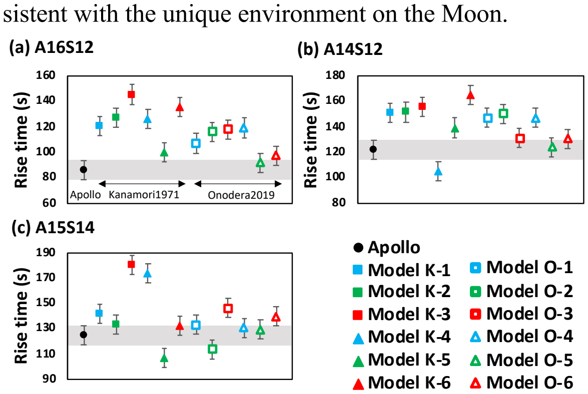

Figure 1. Rise Times for Apollo and Simulated Waves
Rise times with 7.5 s error bars are exhibited for each case (a: Apollo 16 S-IVB received at Station12, termed as A16S12, b: A14S12, c: A15S14).

Next, for the models whose rise-times are comparable to the Apollo data, we calculated the equivalent energy density (EED) defined as equation (1),

$$EED = \sum_{t=0}^{T_{rise}} A_{env}(t)^2 \Big/ T_{rise} \qquad (1)$$

where $A_{env}(t)$ represents the scaled amplitude of the smoothed envelope and T_{rise} shows rise time for each case. Table 4 exhibits the EEDs of the 2 best models for each simulation case in term of energy, normalized with those of the corresponding Apollo ones. The station receives about 85% seismic energy of the Apollo in the case of A14S12 whereas A16S12 and A15S14 cases get nearly 70%. From these results, it is considered that the assumed velocity structure might be a representative for the A14S12 path mainly traveling Mare Cognitum region. Looking at Figure 2, since Model O-6 runs short of energy at the first 60 seconds, Model O-3 seems more preferable to explain the data.

In summary, our results indicate that (i) the smaller V_p/V_s ratio (1.2-1.4) than those proposed by past studies well explains the Apollo rise time, (ii) megaregolith layer exists up to 10 km depth with 7.5 km thick regolith layer in the Mare Cognitum.

Table 4. Equivalent Energy Density for Each Case

Event	Model	EED_{Sim}/EED_{Apo}
A16S12	Model K-5	0.67
	Model O-6	0.71
A14S12	Model O-3	0.86
	Model O-6	0.83
A15S14	Model O-5	0.70
	Model O-6	0.65

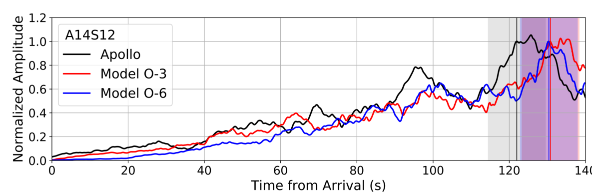

Figure 2. Smoothed Envelopes for A14S12 Best Cases
Each colored envelope shows smoothed envelopes of Apollo (black), Model O-3 (red) and Model O-6 (blue) respectively. Envelopes are normalized with amplitude at each rise time. Colored vertical lines with shade indicate rise time arrival with error of 7.5 s.

Acknowledgments: We would like to thank Lunar and Planetary Exploration Data Analysis Group of ISAS/JAXA, and Research of Interior Structure and Evolution of Solar System Bodies Project of NAOJ for providing us calculation resources. The Apollo seismic data used in this study was collected from Data Archives and Transmission System (DARTS) by the Center for Science-satellite Operation and Data Archive (C-SODA) of ISAS/JAXA.

References: [1] Nakamura et al. (1982), *Proc. LPSC*, *13th*, 117-12. [2] Lognonné et al. (2003), *EPSL*, *211*, 27-44. [3] Garcia et al. (2011), *PEPI*, *188*, 96-113. [4] Blanchette-Guertin et al. (2012), *JGR*, *117*, E06003. [5] Maeda et al. (2017), *EPS*, 69:102. [6] Kanamori et al. (1971), *Proc. 2nd LSC*, *3,* 2323-2326. [7] Onodera et al. (2019), *Proc. LPSC*, *50th*, 1692. [8] Toksoz et al. (1972), *RGSP*, *12*, 539-567. [9] Lee (2003), *U.S. GSB*, 2197. [10] Nakamura and Koyama (1982), *JGR*, *87(B6)*, 4855-4861. [11] Wieczorek et al. (2013), *Science*, *339*, 671-675. [12] Gillet et al. (2017), *PSPI*, *262*, 28-40.